Published in final edited form as:
Bioorg Med Chem Lett. 2011 September 1; 21(17): 4980–4984. doi:10.1016/j.bmcl.2011.05.044.

Deciphering Glycan Linkages Involved in Jurkat Cell Interactions with Gold-coated Nanofibers via Sugar-Displayed Thiols

Jian Du[a,b], **Pao-Lin Che**[a,b], **Udayanath Aich**[b], **Elaine Tan**[b], **Hyo Jun Kim**[b], **Srinivasa-Gopalan Sampathkumar**[c], and **Kevin J. Yarema**[*,b]
Department of Biomedical Engineering and the Translational Tissue Engineering Center, The Johns Hopkins University, Baltimore, MD

Abstract

Metabolic oligosaccharide engineering (MOE) provides a method to install novel chemical functional groups into the glycocalyx of living cells. In this paper we use this technology to compare the impact of replacing natural sialic acid, GalNAc, and GlcNAc with their thiol-bearing counterparts in Jurkat and HL-60 cells. When incubated in the presence of gold-coated nanofibers, only Jurkat cells incubated with Ac_5ManNTGc – an analogue that installs thiols into sialosides – experienced a distinctive "spreading" morphology. The comparison of Ac_5ManNTGc with Ac_5GalNTGc and Ac_5GlcNTGc in the two cell lines implicated sialosides of *N*-linked glycans as critical molecular mediators of the unusual responses evoked in the Jurkat line.

Keywords

Metabolic oligosaccharide engineering; sialic acid; *N*-acetylgalactosamine; *N*-acetylglucososamine; 3D cell culture

This paper describes a step towards the characterization of an unusual morphological response observed in Jurkat cells subject to metabolic oligosaccharide engineering (MOE) when incubated on 3D scaffolds. MOE refers to a technique pioneered by the Reutter group where analogues of *N*-acetyl-D-mannosamine (ManNAc) intercept the sialic acid biosynthetic pathway and are presented on the cell surface as the corresponding non-natural forms of neuraminic acid (Neu5Ac).[1, 2] The Bertozzi group extended MOE by including functional groups not normally found in the glycocalyx – such as the ketone[3] or azide[4] – into analogue design. MOE offers intriguing biomedical opportunities; for example in cancer treatment where non-natural *N*-propionyl or *N*-phenylacetyl derivatives of sialyl Tn prime the immune system to eradicate tumors[5, 6] while analogues bearing bioorthogonal functional groups can serve as a chemical handles for the delivery of a second

[*]Corresponding Author: Translational Tissue Engineering Center, 5029 Robert H. & Clarice Smith Building, The Johns Hopkins University, 400 North Broadway, Baltimore, Maryland USA, kyarema1@jhu.edu, Phone: (1)410.614.6835, Fax: (1)410.614.6840.
[a]These authors contributed equally to this work
[b]Department of Biomedical Engineering, The Johns Hopkins University
[c]Current affiliation: Laboratory of Chemical Glycobiology, National Institute of Immunology Aruna Asaf Ali Marg, New Delhi 110067 India

Supporting Information
Supporting information associated with this article can be found in the online version (doi to be determined).

chemotherapeutic agent.[3] In complementary efforts, we have developed short chain fatty acid (SCFA) derivatized MOE analogues that have improved metabolic efficiency[7] and novel "whole molecule" anti-cancer activities.[8–11]

To facilitate the translation of potential MOE-based therapies from the bench to the bedside, we are developing 3D cell culture models that have been advocated as superior to 2D culture conditions for mimicking *in vivo* tumorigenicity, migration, and metastatic potential.[12, 13] To briefly describe a feature of 3D topography not seen under conventional culture conditions, we recently showed that Jurkat cells – a T-lymphoma derived line that is normally non-adhesive under conventional culture conditions – becomes adherent when grown in the presence of electrospun polyethersulfone (PES) fibrous scaffolds that roughly mimic the architecture of the extra-cellular matrix (Scheme 1A, panels (i) and (ii)). In addition to this topography-driven gain of adhesion, when peracetylated *N*-thiolglycolyl-D-mannosamine (Ac_5ManNTGc) was used to endow cell surface sialic acids with thiol groups,[14] the cells gained a distinctive "spreading" morphology when grown on gold-coated nanofibrous substrate (Fig. 1A, panel (iii)).[15]

Rather remarkably, the blood cell-derived Jurkat cell line – when subjected to 3D topographical cues provided by the microenvironment in combination with the "glycoengineered" binding interface (i.e., the sialic acid presented thiols binding to the gold surface) – began secreting ECM components (e.g., sulfated GAGs).[15] In order to identify specific molecules involved in mediating this cellular response, we designed the novel thiol-bearing analogues Ac_5GalNTGc and Ac_5GlcNTGc (Scheme 1B) to target the *N*-acetyl-D-galactosamine (GalNAc) and *N*-acetyl-D-glucosamine (GlcNAc) salvage pathways, respectively. These experiments were intended to probe whether the presence of a chemical tag located *anywhere* in a surface glycan could elicit the spreading phenomenon or whether the response was unique to sialosides (as illustrated in Figure 1B). In addition, by comparing two immune-derived cancer cell lines, T-lymphoma-derived Jurkat cells and HL-60 human promyelocytic leukemia cells, we reasoned that insight could be gained into whether *N*-glycans (which are primarily expressed by Jurkat cells[16, 17]) or *O*-glycans (which are prevalent in HL-60 cells) predominantly contributed to the unique "spreading" response shown in Scheme 1A.

As an initial step in the evaluation of the thiolated hexosamine analogues Ac_5ManNTGc, Ac_5GalNTGc, and Ac_5GlcNTGc (Scheme 1B), the metabolism of these analogs was characterized in Jurkat and HL-60 cells in order to maximize presentation of cell surface thiols (CSTs, shown in Figure 1C & D) while minimizing or avoiding cytotoxicity (Figure 1A & B). In both Jurkat and HL-60 cells, Ac_5ManNTGc was a more potent analogue than Ac_5GalNTGc or Ac_5GlcNTGc, reaching maximal levels of CST expression at ~25 μM; at higher concentrations the analogues were growth inhibitory (but not actually cytotoxic). Accordingly, 25 μM Ac_5ManNTGc was used in subsequent experiments. By contrast, Ac_5GalNTGc showed only minor growth inhibition up to ~100 μM while maximizing CST display in HL-60 cells (with close to maximal levels also occurring at this concentration in Jurkat cells); accordingly, 100 μM Ac_5GalNTGc was used in subsequent experiments. Unlike the other two analogues, Ac_5GlcNTGc did not increase CST levels above the ethanol control (ethanol is the solvent vehicle in which the sugars were dissolved and all the fluorescence intensities were normalized to this control) even at concentrations up to 200 μM (data not shown). This lack of surface expression is consistent with previous reports which suggest *N*-modified GlcNAc analogues (e.g., Ac_4GlcNAz in Jurkat cells[18]) are partitioned into nucleocytosolic O-GlcNAc but not into surface-displayed *N*-glycans.

Once optimized conditions were determined for CST expression using Ac_5ManNTGc and Ac_5GalNTGc, quantification of cell attachment showed that these two analogues enhanced

attachment to gold-coated nanofibers compared to Ac_5GlcNTGc-treated cells (results not shown). These results are consistent with a lack of high affinity thiol-gold interactions between the glycocalyx of the cells incubated with the GlcNAc analogue and the chemically compatible growth substrate; Ac_5GlcNTGc therefore was not used further in these experiments. For Ac_5ManNTGc- and Ac_5GalNTGc-treated cells that did display enhanced levels of CSTs, the Jurkat line – which is rich in *N*-linked glycoproteins – displayed cell spreading morphology that resembled basement membrane when treated with Ac_5ManNTGc but not with Ac_5GalNTGc (Figure 2). Conversely, the HL-60 cells, which are rich in *O*-linked glycoproteins, showed no morphology change when treated with either Ac_5ManNTGc or Ac_5GalNTGc.

The results shown in Figure 2 implicate thiolated sialosides present in *N*-glycans is critical for the spreading morphology observed in Ac_5ManNTGc-treated Jurkat cells incubated on gold coated nanofibers. To gain further support for the hypothesis that the basement membrane-like morphology seen in these cells was induced by non-natural thiol-bearing sialic acids borne by *N*-linked glycoproteins, we conducted a series of studies designed to further modulate sialoside and CST expression in Ac_5ManNTGc-treated cells and then evaluated the response of these cells when grown on 3D gold-coated scaffolds. First, because the extracellular milieu in tissue culture is slightly oxidizing, a large proportion of the sialic acid displayed thiols form disulfide linkages.[19] We therefore used tris(2-carboxyethyl)phosphine hydrochloride (TCEP; a mild disulfide-reducing agent) to reduce disulfides before the cells were cultured on gold coated PES nanofibers. In flow cytometry assays (as described previously[14, 19]), TCEP treatment of Ac_5ManNTGc-incubated cells increased reagent-accessible CST levels from ~5.5 to 18-fold above background levels (Figure 3A). When cells were treated with both Ac_5ManNTGc and TCEP and then cultured on gold-coated nanofibers, the enhanced accessibility of the thiols groups increased the base membrane-producing, spreading morphology of the cells (Figure 3B, panel (ii)) compared to those only incubated with Ac_5ManNTGc (panel (i)).

To further confirm the role of thiol-modified sialic acids in the Jurkat cell response, sialidase (or neuraminidase, EC 3.3.3.18) was used to cleave sialic acid residues from the oligosaccharide moieties of glycoproteins and glycolipids. Because Ac_5ManNTGc intercepts the sialic acid biosynthetic pathway to express Neu5TGc on the cell surface, we postulated that sialidase would modestly reduce CST expression by removing the 5 to 10% of non-disulfide linked Neu5TGc (we have previously shown that >90% of CST expression arising from Ac_5ManNTGc treatment exists in the oxidized form[14, 19] and we consider it to be unlikely that sialidase would cleave these disulfide-linked sialosides). Consistent with this premise, the decreased CST levels in cells treated with sialidase (Figure 3A) resulted in a sharp decrease in spreading morphology of sialidase-treated cells (Figure 3B, panel (iii)) compared with the Ac_5ManNTGc-treated controls (panel (i)).

As a final verification that *N*-glycans were implicated in the spreading phenomenon, the effects of tunicamycin (which inhibits UDP-GIcNAc:Dolichyl-P-GlcNAc-1-P-transferase and thereby reduces *N*-linked glycosylation) on CST display and morphology of Ac_5ManNTGc-treated Jurkat cells were analyzed. When Jurkat cells were pre-treated with tunicamycin before they were incubated with Ac_5ManNTGc, there was a significant reduction in thiol expression levels compared to Ac_5ManNTGc treatment only (5.5 vs. 1.9, Figure 3A) and SEM showed an absence of the “spreading” morphology observed in the tunicamycin-untreated cells (Figure 3B). Together, these experiments provide compelling evidence that the unique spreading morphology of the Jurkat cells is plausibly explained by the interaction between the 3D nanofiber gold substrate and the non-natural thiol groups expressed specifically in sialosides of the *N*-linked glycoproteins.

The broader implications of the work described in this brief report are several-fold. First, hematopoietic cancer cells respond to 3D topographical cues, with both the Jurkat and HL-60 lines becoming adherent upon incubation with nanofibrous scaffolds. Further, cell responses can be enhanced by the creation of a “glycoengineered” binding interface; specifically new types of high affinity, carbohydrate-based adhesion between thiols newly-expressed in cell surface glycans interact with the gold substrate to provoke very unusual morphological and biochemical responses in Jurkat cells. At the same time, because such responses were not observed in HL-60 cells, this study sets the stage for control of specific cell types in situations where multiple cell types co-exist (e.g., in the human body). Perhaps most significantly, the use of the novel analogues Ac_5GalNTGc and Ac_5GlcNTGc demonstrated that these responses were not due to glycans in general, but rely on sialic acids in particular which is consistent with the emerging paradigm that MOE can be used to modulate signaling pathways engaged by sialic acids.[20]

Supplementary Material

Refer to Web version on PubMed Central for supplementary material.

Acknowledgments

Funding for this study was provided by the National Institutes of Health (NIBIB, EB005692-04) and SGS thanks the Department of Biotechnology (DBT), Government of India for the Ramalingaswami Fellowship.

References

1. Kayser H, Zeitler R, Kannicht C, Grunow D, Nuck R, Reutter WJ. Biol. Chem. 1992; 267:16934.
2. Du J, Meledeo MA, Wang Z, Khanna HS, Paruchuri VD, Yarema KJ. Glycobiology. 2009; 19:1382. [PubMed: 19675091]
3. Mahal LK, Yarema KJ, Bertozzi CR. Science. 1997; 276:1125. [PubMed: 9173543]
4. Saxon E, Bertozzi CR. Science. 2000; 287:2007. [PubMed: 10720325]
5. Chefalo P, Pan Y, Nagy N, Guo Z, Harding CV. Biochemistry. 2006; 45:3733. [PubMed: 16533056]
6. Wu J, Guo Z. Bioconjug. Chem. 2006; 17:1537. [PubMed: 17105234]
7. Kim EJ, Sampathkumar S-G, Jones MB, Rhee JK, Baskaran G, Yarema KJ. J. Biol. Chem. 2004; 279:18342. [PubMed: 14966124]
8. Aich U, Campbell CT, Elmouelhi N, Weier CA, Sampathkumar S-G, Choi SS, Yarema KJ. ACS Chem. Biol. 2008; 3:230. [PubMed: 18338853]
9. Campbell CT, Aich U, Weier CA, Wang JJ, Choi SS, Wen MM, Maisel K, Sampathkumar S-G, Yarema KJ. J. Med. Chem. 2008; 51:8135. [PubMed: 19053749]
10. Elmouelhi N, Aich U, Paruchuri VDP, Meledeo MA, Campbell CT, Wang JJ, Srinivas R, Khanna HS, Yarema KJ. J. Med. Chem. 2009; 52:2515. [PubMed: 19326913]
11. Wang Z, Du J, Che P-L, Meledeo MA, Yarema KJ. Curr. Opin. Chem. Biol. 2009; 13:565. [PubMed: 19747874]
12. Dhiman HK, Ray AR, Panda AK. Biomaterials. 2005; 26:979. [PubMed: 15369686]
13. Kim YJ, Bae HI, Kwon OK, Choi MS. Int. J. Biol. Macromol. 2009; 45:65. [PubMed: 19375451]
14. Sampathkumar S-G, Li AV, Jones MB, Sun Z, Yarema KJ. Nat. Chem. Biol. 2006; 2:149. [PubMed: 16474386]
15. Du J, Che P-L, Wang Z-Y, Aich U, Yarema KJ. Biomaterials. 2011 Epub ahead of print: http://dx.doi.org/10.1016/j.biomaterials.2011.04.005.
16. Piller V, Piller F, Fukuda M. J. Biol. Chem. 1990; 265:9264. [PubMed: 2140570]
17. Yarema KJ, Mahal LK, Bruehl RE, Rodriguez EC, Bertozzi CR. J. Biol. Chem. 1998; 273:31168. [PubMed: 9813021]

18. Vocadlo DJ, Hang HC, Kim E-J, Hanover JA, Bertozzi CR. Proc. Natl. Acad. Sci. U.S.A. 2003; 100:9116. [PubMed: 12874386]
19. Sampathkumar S-G, Jones MB, Yarema KJ. Nat. Protoc. 2006; 1:1840. [PubMed: 17487167]
20. Kontou M, Weidemann W, Bork K, Horstkorte R. Biol. Chem. 2009; 390:575. [PubMed: 19361277]
21. Sampathkumar S-G, Li AV, Yarema KJ. Nat. Protoc. 2006; 1:2377. [PubMed: 17406481]

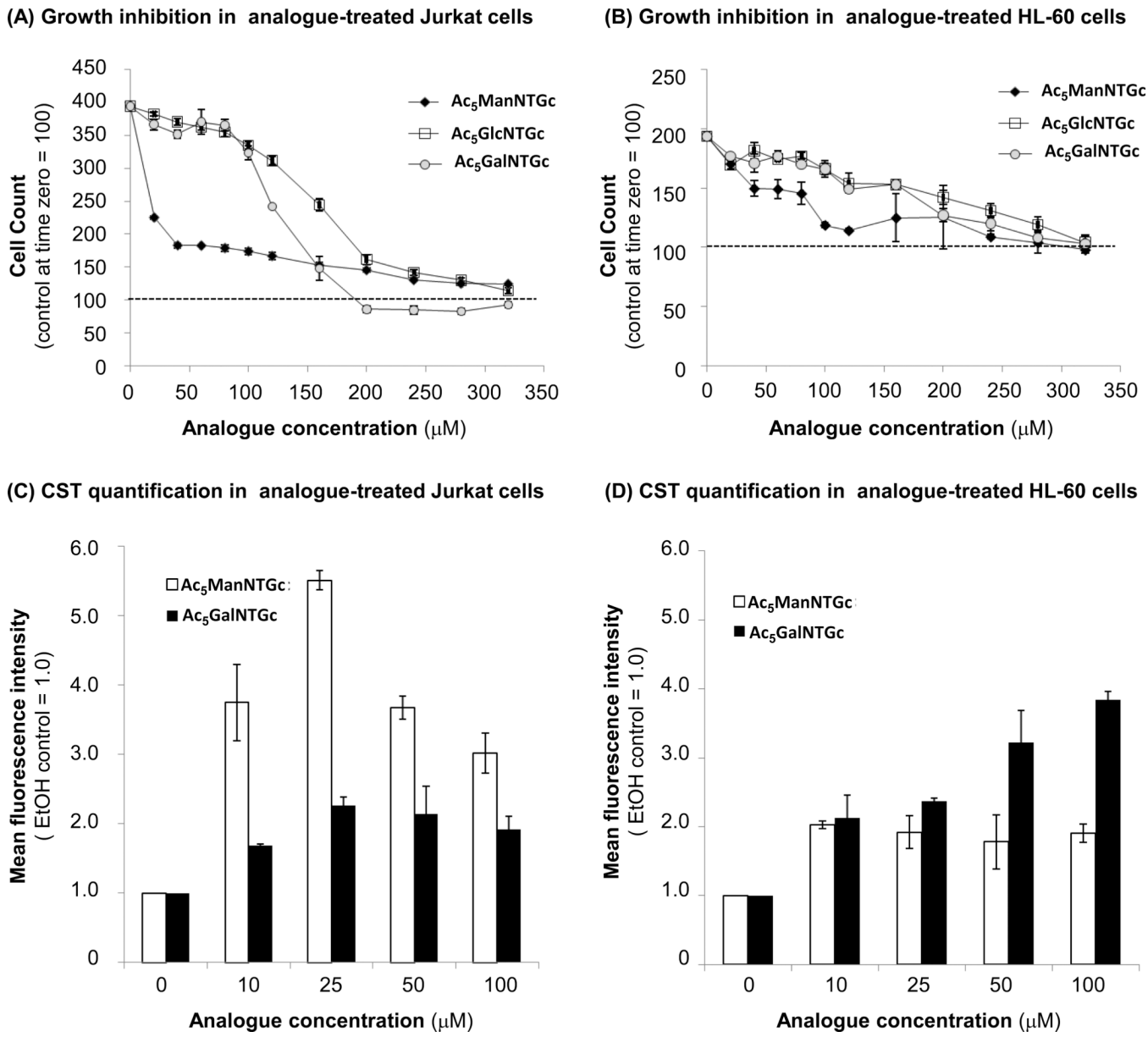

Figure 1.

Characterization of growth inhibition (Panels A & B) and metabolic incorporation into surface glycans (Panels C & D) of thiolated hexosamine analogues in Jurkat (Panels A & C) and HL-60 (Panels B & D). Growth inhibition in Ac_5ManNTGc-, Ac_5GlcNTGc-, and Ac_5GalNTGc-treated cells was measured after 48 h by taking cell counts. The data shown are the mean ± SD of three independent replicates compared to the initial number of cells present in each culture (e.g., values ≥100 represent net cell proliferation while numbers ≤100 indicate cell death has occurred). Cell surface thiol (CST) expression for Jurkat and HL-60 cells treated with Ac_5ManNTGc and Ac_5GalNTGc for 48 h was measured by a flow cytometry assay using published protocols.[14, 19] EtOH control assigned a MFI value of 1.0. Data shown are the mean ± SD of three independent replicates. (MFI = mean fluorescence intensity). The CST levels measured for Ac_5GlcNTGc treated cells were statistically identical to the EtOH control (not shown).

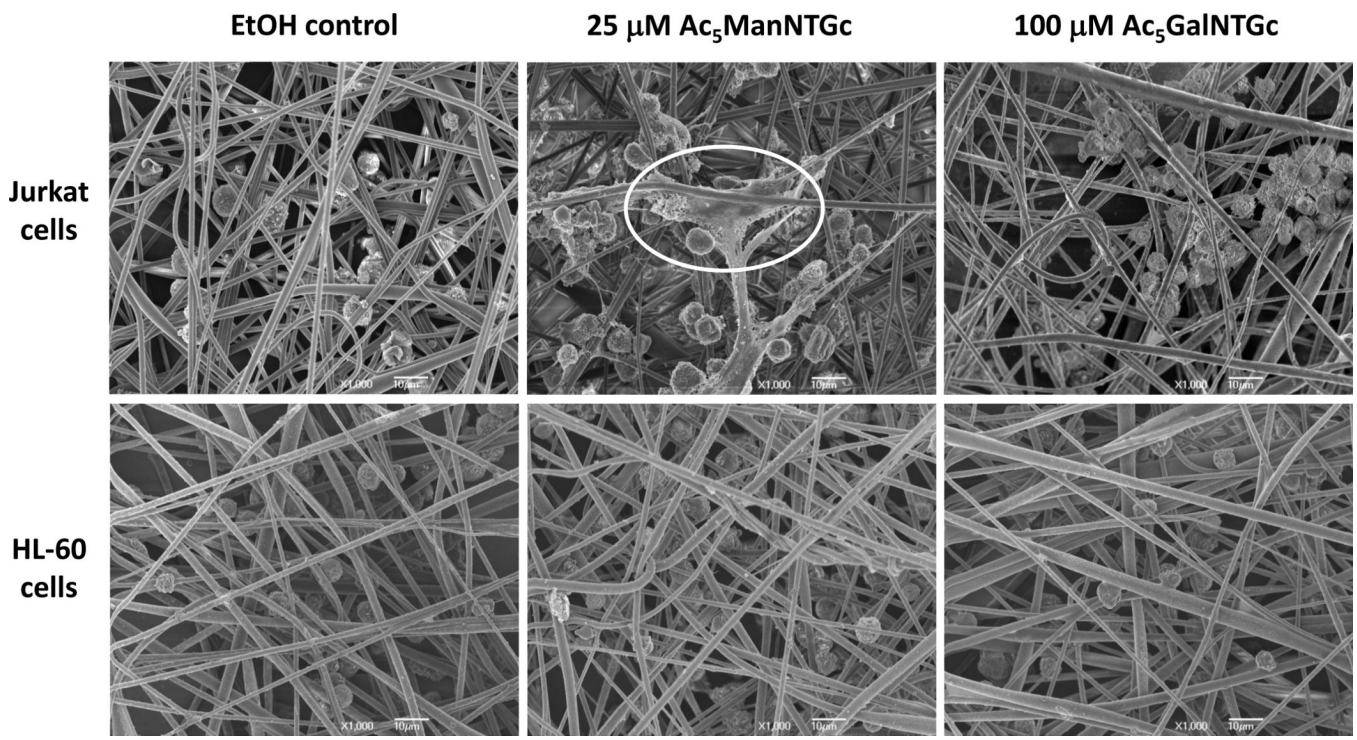

Figure 2.

SEM micrographs of Jurkat and HL-60 cells cultured with EtOH as the negative control, 25 μM Ac_5ManNTGc, and 100 μM Ac_5GalNTGc for 48 h and then incubated on gold coated fibrous scaffolds. Of note, the HL-60 cells (grow in suspension under normal culture conditions in a manner similar to Jurkat cells, see Scheme 1A) became attached to the fibers when presented with 3D topology but under no conditions assumed the “spreading” morphology highlighted in the top center panel for Jurkat cells. The electrospun nanofibers used in this experiment were previously optimized for layer thickness (~50 μM), gold coating (~20 nm), and diameter (1012 nm).[15]

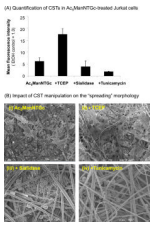

Figure 3.

The effect of TCEP, sialidase, and tunicamycin treatment on surface thiol expression and "spreading" morphology in Jurkat cells. (A) Cells were treated with 25 μM Ac_5ManNTGc for 48 h (and in all cases compared to an EtOH-treated control, which was assigned a MFI value of 1.0) and analyzed for CST expression[19] (i) without further treatment, (ii) after TCEP treatment (1.0 mM for 1.0 h, as described elsewhere[19]), or (iii) after Sialidase EC 3.3.3.18 (*Vibrio cholera*, Sigma-Aldrich) treatment (75 mU sialidase was used to treat 10^6 cells in 1.0 mL for 1.0 h at 37°C). (iv) Alternately, cells were pretreated with 0.45 μg/ml tunicamycin for 24 h prior to addition of Ac_5ManNTGc and then incubated with analogue for 48 h before analysis. Data shown are the mean ± SD of three independent replicates. (B) SEM micrographs of Jurkat cells pretreated with 25 μM Ac_5ManNTGc followed by incubation (i) on gold-coated PES fibrous scaffold without further manipulation or after (ii) TCEP or (iii) sialidase treatment; finally, (iv) and tunicamycin pre-treated cells were cultured on the gold coated PES fibrous scaffold.

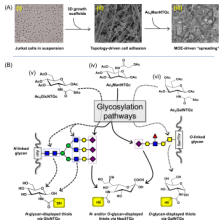

Scheme 1.

(A) Overview of topography and MOE in the behavior and *in vitro* study of cancer cells. (i) Jurkat cells grow in suspension under normal tissue culture conditions but (ii) become adherent – but otherwise appear normal – in the presence of growth scaffolds with 3D topography that mimics micro-architectural features of the ECM. (iii) Adding the contributions of MOE by installing thiols in the glycocalyx via Ac_5ManNTGc results in a unique and distinctive "spreading" morphology when the cells are grown on gold coated nanofibers. (B) Dissecting the submolecular glycan feature(s) responsible for the Jurkat spreading morphology. Ac_5ManNTGc (iv, center) is converted to the thiolated sialic acid "Neu5TGc" that can be incorporated into both *N*-linked and *O*-linked glycans. To further probe which class of glycan was responsible for Jurkat spreading morphology, Ac_5GlcNTGc (v, left) and Ac_5GalNTGc (vi, right) were synthesized and tested; the former analogue was designed to be incorporated into *N*-glycans to replace GlcNAc and the latter into *O*-glycans as a replacement for GalNAc. Note that Ac_5ManNTGc was synthesized and characterized as reported previously[21] while the synthesis and characterization of Ac_5GalNTGc and Ac_5GlcNTGc are described in the Supporting information.